Carbohydrate Polymers 152 (2016) 33–40

Contents lists available at ScienceDirect

Carbohydrate Polymers

journal homepage: www.elsevier.com/locate/carbpol

# Structure elucidation of a non-branched and entangled heteropolysaccharide from *Tremella sanguinea* Peng and its antioxidant activity

Zhaojing Wang, Yawei Zeng, Dianhui Luo *

*Huaqiao University, Department of Bioengineering and Biotechnology, Xiamen, 361021, China*

ARTICLE INFO

*Article history:*
Received 18 May 2016
Received in revised form 20 June 2016
Accepted 24 June 2016
Available online 25 June 2016

*Keywords:*
*Tremella sanguinea* Peng
Structural analysis
TEM

ABSTRACT

A crude polysaccharide was extracted from the edible fungi *Tremella sanguinea* Peng, and a polysaccharide TSP-II (31.56%) was separated and purified from the crude polysaccharide. TSP-II was a homogeneous polysaccharide by the high-performance size-exclusion chromatography (HPSEC), had a molecular weight of 356 kD and consisted mainly of mannose, xylose, galactose and glucose at a molar ratio 5.9:2.4:1:1.1. The structural assignment of TSP-II was carried out using fourier transform infrared spectroscopy (FTIR) analysis, periodate oxidation-smith degradation, partial hydrolysis with acid, methylation analysis and nuclear magnetic resonance (NMR) studies, and the repeating unit of TSP-II was thus determined. The result indicated that →3)-α-D-Man*p*-(1→, →2)-α-D-Xyl*p*-(1→, →6)-α-D-Glc*p*-(1→ and →3)-α-D-Gal*p*-(1→ formed the major components of the main-chain structure, and TSP-II was a non-branched polysaccharide. Transmission electron microscopy (TEM) analysis revealed a primary non-branched and entangled state in its microstructure. TSP-II had higher scavenging activities on hydroxyl radical ($EC_{50}$ = 0.088 mg/ml) and superoxide radical ($EC_{50}$ = 0.127 mg/ml) than Vitamin C (Vc).



## 1. Introduction

*Tremella* species are well known as the traditional edible fungi in oriental countries. The species from this family mainly include *Tremella fuciformis Berk., Tremella aurantialba Bandoni et Zang and Tremella encephala Pers*. The polysaccharides from these species exhibited numerous potent biological and pharmacological functions and had attracted much attention and research (Wang, Qu, Chu, Li, & Tian, 2002; Zhang, Qu, & Zhang, 2004; Du et al., 2009; Kiho et al., 2001). *Tremella samguinea* Peng, known as Xue'er in China, is a new species from *Tremella* family identified in 1990 (Peng, 1990), and it has been mainly used as food. Nowadays, the research on polysaccharides from *T. samguinea* Peng is less compared to other species from *Tremella* family (Xie & Hu, 1992 Liu & Guo, 2009).

In our previous work, the antioxidant activity of several crude polysaccharide fractions from *Tremella* family had been reported (Luo & Zeng, 2014). Several products were extracted from four fungi of *Tremella* family, and two extracts TSPA and TSPW from *T. samguinea* Peng exhibited the highest scavenging activities of hydroxyl radical and superoxide radical. Polysaccharide structure should be determined to further investigate the relationship between the chemical structures and biological activities of polysaccharides from *T. samguinea* Peng. However, the physicochemical properties and the detailed chemical structure of polysaccharides purified from *T. samguinea* Peng have not been investigated, and the structure-function relationship has yet been established. This situation significantly restricts the further development of *T. samguinea* Peng in other fields, including the energy, medical and food industries.

In the present study, a polysaccharide, named TSP-II, was isolated from *T. samguinea* Peng, and the chemical structure and the antioxidant activity of TSP-II were investigated. To our knowledge, this is the first time that detailed structure was performed on polysaccharides from *T. samguinea* Peng.

## 2. Materials and methods

### 2.1. Materials and chemicals

*T. sanguinea* Peng was purchased from a local store (Shennongjia, Hubei Province, China). The material was identified by Professor J. F. Liu, Huaqiao University, Fujian, China. Monosaccharide samples (Sigma Co., St Louis, MO, USA), dextran standard samples (Sigma Co., St Louis, MO, USA) and Deuterium Oxide ($D_2O$,

* Corresponding author.
*E-mail addresses:* dianhuiluo@163.com, luodhwzj@hqu.edu.cn (D. Luo).

http://dx.doi.org/10.1016/j.carbpol.2016.06.094
0144-8617/

Cambridge Isotope Laboratories, Inc., Andover, MA, USA) were purchased from a local agent (Taijing Co., Xiamen), while DEAE Sepharose CL–6 B was acquired from Pharmacia Co. (Sweden). All other reagents used were of analytical grade.

### 2.2. Isolation and purification of polysaccharide

Dry *T. sanguinea* Peng (100 g) was extracted with $1.2 \times 10^4$ mL distilled water at 100 °C for 120 min. The extracts were concentrated and kept overnight at 4 °C to precipitate polysaccharides with four volumes of ethanol. The precipitate was collected and dried in a freeze drier to produce a crude polysaccharide. The crude polysaccharide (500 mg) was dissolved in 10 mL distilled water and injected into a column (4.6 cm × 40 cm) of DEAE-Sepharose CL-6B. The column was eluted with distilled water at 50 mL/h (12 min/tube), followed by NaCl aqueous solution (0–1 M) for 500 mL. The polysaccharide fractions were collected with a fraction collector, dialyzed (MWCO 3500) against distilled water for 48 h and dried in a freeze drier to produce purified polysaccharides.

### 2.3. Homogeneity and properties determination

Total content of polysaccharides was determined by phenole-sulfuric acid method (Dubois, Gillis, Hamilton, Rebers, & Smith, 1956). The concentration of proteins was measured according to Bradford's method (Bradford, 1976).

The homogeneity and the molecular weight (MW) of polysaccharides were determined by high-performance size-exclusion chromatography (HPSEC) (1100 system, Agilent Technologies, Palo Alto, CA, USA) with a gel-filtration chromatographic column of Shodex Sugar KS-804 (Showa Denko K.K, Japan) and a refractive index detector (RID). The molecular weight was calculated by a calibration curve obtained by using various standard dextrans of different molecular weights (Dextran Blue, Dextran T10, T40, T70, T500 and Glucose) (Luo & Fang, 2008; Wang, Zhou, & Quan, 2014).

Gas chromatography (GC) and high-performance liquid chromatography (HPLC) were used for the identification and quantification of monosaccharide composition. For GC analysis, the polysaccharide (10 mg) was dissolved in 1 mL of 1 M HCl-Methanol, and derivation was then carried out using the trimethylsilylation reagent (Wang & Luo, 2007). The monosaccharide composition was analyzed on a gas chromatography system (6890 system, Agilent Technologies, Palo Alto, CA, USA) equipped with an HP-5 column (30 m × 0.25 mm × 0.25 μm) and a flame-ionization detector (FID) (Luo & Fang, 2008).

For HPLC analysis, the purified polysaccharide (80 mg) was hydrolyzed with 1 M $H_2SO_4$ and kept at 100 °C for 8 h. The content was neutralized to pH 7.0 with barium carbonate, filtrated, concentrated and freeze-dried. It was then applied to a gel-filtration chromatographic column of Shodex Sugar SP0810 (Showa Denko K.K, Japan), maintained at a temperature of 80 °C, eluted with distilled water at a flow rate of 0.5 mL/min and detected by a refractive index detector (RID).

FTIR spectrum of the polysaccharide was determined using a Fourier Transform Infrared Spectrometer (Nicolet iS10, Thermo Fisher Scientific, Waltham, MA, USA). The purified polysaccharide (1–2 mg) was ground with 0.2 mg KBr powder and then pressed into pellets for FTIR measurement at a frequency range of 4000–400 $cm^{-1}$ (Kumar, Joo, Choi, Koo, & Chang, 2004).

### 2.4. Periodate oxidation-Smith degradation

For analytical purposes, 50 mg of the polysaccharide was dissolved in 25 mL of distilled water, and 25 mL of 30 m mol/L $NaIO_4$ was added. The solution was kept in the dark, and 0.2 mL aliquots were withdrawn at 6 h intervals, diluted to 50 mL with distilled water and read at 223 nm. Glycol (2 mL) was added, the solution of periodate product (2 mL) was sampled to calculate the yield of formic acid by 0.005 M sodium hydroxide, and the rest was extensively dialyzed against tap water and distilled water for 24 h, respectively. The content was concentrated and reduced with $NaBH_4$ (80 mg) at room temperature for 24 h, neutralized to pH 6.0 with 50% acetic acid, dialyzed as described above and concentrated to a volume of 10 mL. One-third of the solution was freeze-dried and analyzed with GC. The other solution was added to the same volume of 1 M sulfuric acid, kept for 40 h at 25 °C, neutralized to pH 6.0 with barium carbonate and filtered. The filtrate was dialyzed as described, and the content outside of the sack was desiccated for GC analysis. The content inside the sack was diluted with ethanol. After centrifugation, the supernatant and the precipitate were also dried out for GC analysis (Luo et al., 2016; Luo & Fang, 2008).

### 2.5. Partial hydrolysis with acid

The polysaccharide (120 mg) was hydrolyzed with 0.05 M $CF_3COOH$, kept at 95 °C for 16 h and centrifuged. The sediment was dried and used to GC analysis. The supernatant was dialyzed with distilled water for 48 h, and the solution out the sack was dried and used to GC analysis. The solution in the sack was diluted with ethanol, the precipitate and the supernatant were dried, and GC was carried out (Luo et al., 2016).

### 2.6. Methylation and GC–MS analysis

The polysaccharide (30 mg) was methylated twice and examined by FTIR spectrum. No absorption peak of hydroxyl identified the complete methylation. The desiccated methylated polysaccharide was subjected to formic acid, isolated from any excess formic acid with methanol, hydrolyzed in $CF_3COOH$, reduced with $NaBH_4$ and acetylated with acetic anhydride–pyridine (1:1). The resulting methylated alditol acetates were subjected to GC–MS analysis (Luo, 2008). Gas chromatography mass spectrometry (GC–MS) was performed on a HP7890A-5975C instrument (Agilent Technologies, Palo Alto, CA, USA) with an HP–5 ms (30 m × 0.25 mm × 0.25 um) column at temperatures programmed from 160 (held for 1 min) to 250 °C (held for 2 min) at 8 °C/min. The injector temperature and the detector temperature were set at 280 °C, and helium was used as the carrier gas at a rate of 2 mL/min. Linkages were identified on the basis of the relative retention time and the fragmentation pattern (Wang et al., 2001; Komura, Ruthes, Carbonero, Gorin, & Iacomini, 2014; Luo et al., 2016).

### 2.7. Nuclear magnetic resonance (NMR) spectroscopy

For the NMR measurements, 20–30 mg samples were dried in a vacuum over $P_2O_5$ for several days, exchanged with deuterium by lyophilizing with $D_2O$ for three times and then dissolved in 0.7 mL $D_2O$ (99.96%). The $^1H$ and $^{13}C$ NMR spectra experiments were recorded at 500 MHz and 125 MHz on an AVANCE-500 NMR spectrometer (Bruker Inc., Rheinstetten, Germany) at 24 °C. The $^1H$ NMR chemical shifts were referenced using the HOD signal at $\delta$ 4.6 ppm at 24 °C. The 2D NMR experiments were performed using standard Bruker software. The 2D NMR spectra included $^1H/^1H$ homonuclear correlation spectroscopy ($^1H$–$^1H$ COSY), total correlation spectroscopy (TOCSY), heteronuclear single quantum coherence (HSQC), heteronuclear multiple-bond coherence (HMBC) and nuclear overhauser enhancement spectroscopy (NOESY) (Liu, Wen, Kan, & Jin, 2015; Pramanik, Mondal, Chakraborty, Rout, & Islam, 2005; Li, Wei, Sun, & Xu, 2006).

**Table 1**
GC results from fractions of smith degradation and partial acid hydrolysis of TSP-II.

| Fractions | | Sugar components and molar ratios | | | | | |
|---|---|---|---|---|---|---|---|
| | Man[a] | Xyl[b] | Gal[c] | Glc[d] | Gly[e] | Ery[f] | |
| Partial acid hydrolysis | precipitation | 6.9 | 3.4 | 1 | 1.25 | –[h] | – |
| | precipitation in the sack | 3.4 | 1.7 | 1 | 0.23 | – | – |
| | supernatant in the sack | 4.6 | 1.1 | 1 | – | – | – |
| | fraction out of sack | 1.4 | 1.78 | 1 | 0.75 | – | – |
| Smith degradation | full acid hydrolysis | 3.1 | 0.95 | 1 | – | 0.58 | – |
| | out of sack | 1.6 | – | 1 | – | 1.4 | – |
| | supernatant in the sack | +[g] | – | – | – | – | – |
| | precipitation in the sack | 8.5 | 0.23 | 1 | – | 0.4 | – |

[a] Mannose.
[b] Xylose.
[c] galactose.
[d] glucose.
[e] glycerol.
[f] erythritol.
[g] Detectable.
[h] Undetectable.

### 2.8. Microscopic analysis

To observe the microstructure of TSP-II, sodium dodecyl sulfate (SDS) was selected as a surfactant to disperse the polysaccharide in an aqueous solution (Chen, Liu, Zhang, Niu et al., 2015; Chen, Zhang, Chen, & Cheung, 2014). The aqueous solution was prepared at a concentration of 1 mg/ml, followed by the addition of an equal volume of SDS solution (1 mg/ml). The mixture was heated at 80 °C for 2 h, diluted with DD $H_2O$ to a final concentration (5 μg/ml), and then heated to 80 °C for 2 h. A droplet of solution was deposited on the carbon film specimen (200 mesh, Beijing Zhongjingkeyi Technology, Beijing, China). After drying at an ambient temperature, transmission electron microscopy (H-7650, Hitachi High-Technologies Corporation, Tokyo, Japan) with an accelerating voltage of 100 kV was applied to visualize the molecular morphology of the sample (Chen & Cheung, 2014).

### 2.9. Antioxidant activities assay

The superoxide radical assay, the hydroxyl radical assay and the scavenging ability for DPPH were measured by using the methods previously described (Wang & Luo, 2007; Yuan, Zeng, Nie, Luo, & Wang, 2015).

## 3. Results and discussion

### 3.1. Physicochemical properties of TSP-II

The crude polysaccharide (TSP) was isolated from the hot-water extract of *T. sanguinea* Peng, and the extraction conditions were as follows: liquid to solid ratio 120 mL/g, extraction time 210 min and extraction temperature 97 °C. After fractionation by the DEAE-Sepharose CL–6 B (data not shown), TSP gave two major fractions, TSP-II was a fraction from the NaCl aqueous solution, and it was the largest one with a yield of 31.56%. We came to the conclusion that TSP-II was homogeneous with only one symmetrical peak by HPSEC (data not shown) in a Sugar KS-804 column. The average molecular weight of TSP-II was estimated from a calibration curve ($y = -4x + 6.3$) prepared with standard dextrans, and it was nearly 356 kD. TSP-II was composed of approximately 97.3% (w/w) of total carbohydrate, which did not contained uronic acid, and TSP-II showed a trace response of 1.05% to the Bradford test. On hydrolysis by 1 M HCl-Methanol, the presence of mannose, xylose, galactose and glucose in GC analysis (data not shown) was detected. TSP-II derivatives produced after the derivation in GC was not stable, which made it difficult to accurately quantify the ratio of monosaccharide (Niu et al., 2014). To further validate the result from GC analysis and quantify the ratio of monosaccharide, a HPLC analysis was carried out. On hydrolysis by 1 M $H_2SO_4$, the presence of mannose, xylose, galactose and glucose at a molar ratio 5.9:2.4:1:1.1 was detected by HPLC analysis (Fig. 1a). The infrared spectrum

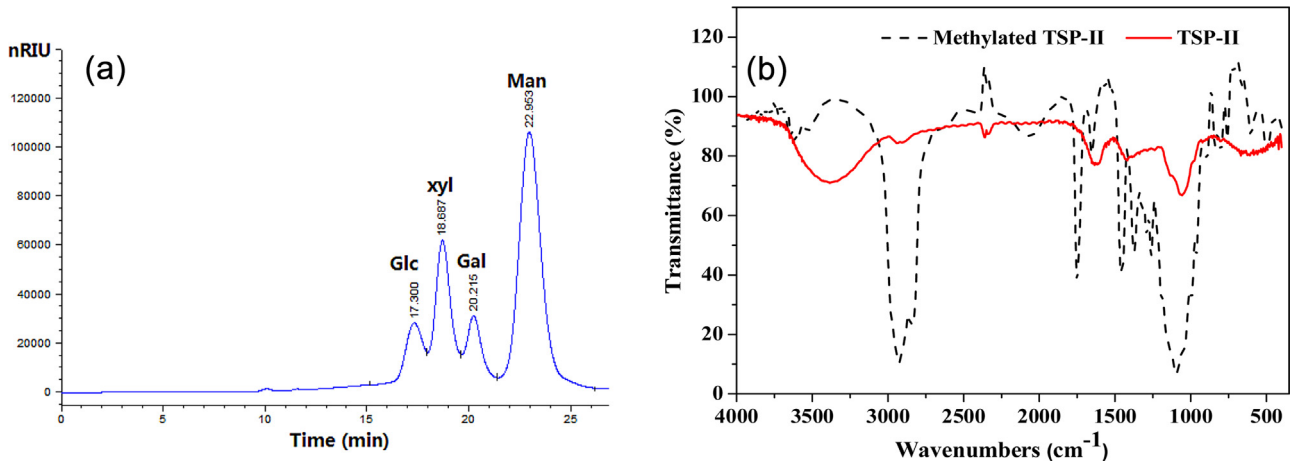


**Fig. 1.** HPLC chromatography of TSP-II on a Shodex Sugar SP-0810 column (a) and IR spectra of TSP-II and methylated TSP-II (b).

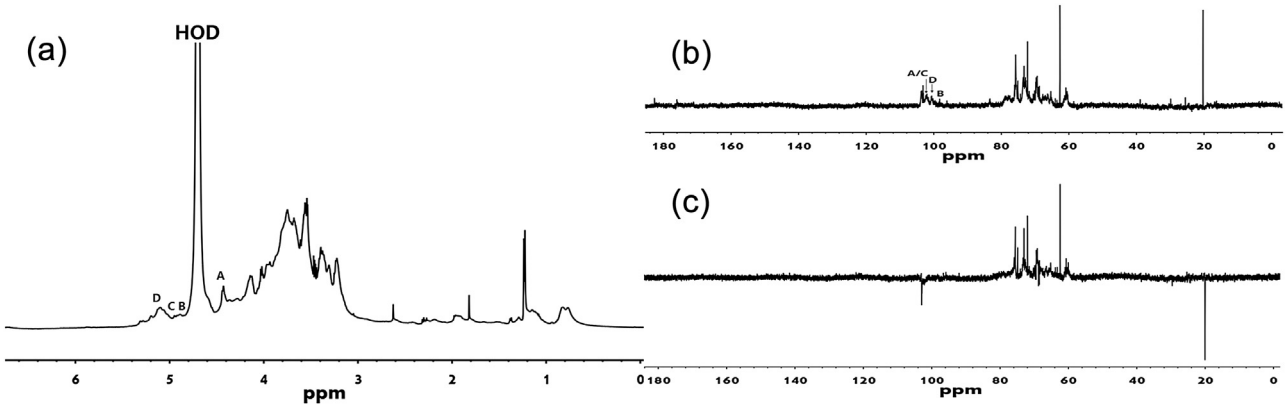


**Fig. 2.** $^{1}$H NMR (500 MHz, $D_2O$, a), $^{13}$C NMR (125 MHz, b) and DEPT135 (c) spectra of polysaccharide TSP-II from *T. samguinea Peng*: the anomeric protons were labeled A-D.

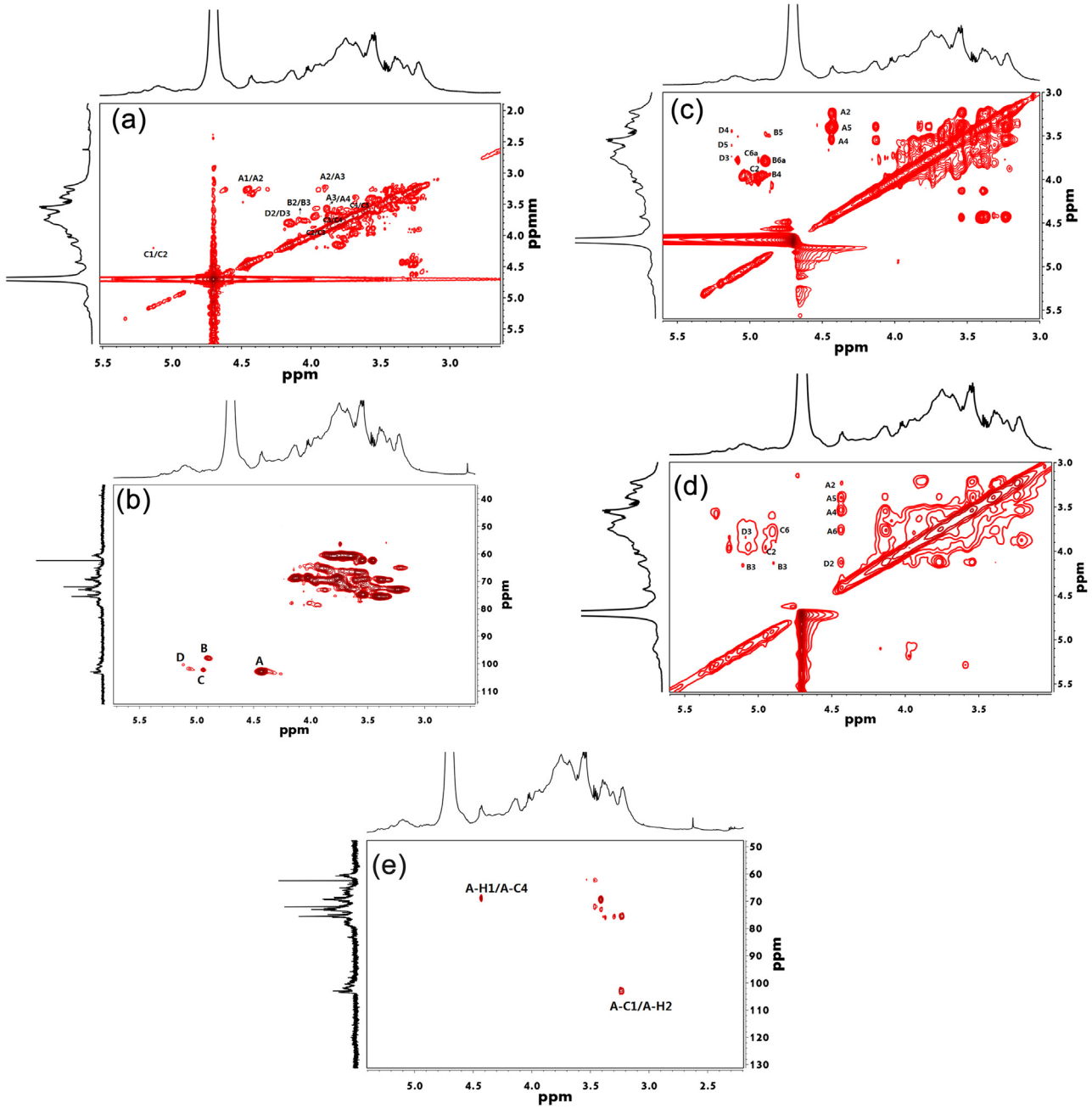


**Fig. 3.** $^{1}$H-H COSY (a), HSQC (b), TOCSY (c), NOESY (d), and HMBC (e) spectrums of polysaccharide TSP-II: the anomeric protons were labeled A-D.

**Table 2**
GC–MS chromatogram of methylated products of TSP-II.

| Methylation product | Molar ratio | Mass fragment (*m*/*z*) | Linkage type |
|---|---|---|---|
| 1,2,5-*O*-Ac3-3,4-*O*-me$_2$-D-xylitol | 0.8 | 43,45,71,87,101,129,161 | 1,2-D-Xyl*p* |
| 1,3,5-*O*-Ac3-2,4,6-*O*-me$_3$-D-galactiol | 1 | 43,45,87,101,117,129,161 | 1,3-D-Gal*p* |
| 1,3,5-*O*-Ac3-2,4,6-*O*-me$_3$-D-mannitol | 4.45 | 43,45,87,101,117,129,161 | 1,3-D-Man*p* |
| 1,5,6-*O*-Ac3-2,3,4-*O*-me$_3$-D-glucitol | 1.31 | 43,87,99,101,117,129,161 | 1,6-D-Glc*p* |

**Table 3**
$^1$H and $^{13}$C chemical shifts of polysaccharide TSP-II recorded in $D_2O$ at 24 °C.

| | | | Chemical shift, δ | | | | | | |
|---|---|---|---|---|---|---|---|---|---|
| No | Glycosyl residue | | 1 | 2 | 3 | 4 | 5 | 6a | 6b |
| A | →3)-α-D-Man*p*-(1→ | H | 4.43 | 3.24 | 3.91 | 3.56 | 3.40 | – | – |
| | | C | 102.8 | 72.6 | 79.0 | 68.8 | 75.3 | | |
| B | →3)-α-D-Gal*p*-(1→ | H | 4.90 | 3.81 | 4.05 | 3.95 | 3.47 | 3.79 | – |
| | | C | 98.1 | 69.8 | 78.6 | 70.1 | 71.3 | 61.8 | |
| C | →6)-α-D-Glc*p*-(1→ | H | 4.94 | 3.98 | 3.87 | 3.68 | 3.45 | 3.78 | – |
| | | C | 102 | 70.5 | 73.6 | 71.8 | 71.1 | 68.9 | |
| D | →2)-α-D-Xyl*p*-(1→ | H | 5.13 | 4.16 | 3.76 | 3.44 | 3.60 | | |
| | | C | 100.4 | 78.1 | 72.8 | 71.4 | 61.8 | | |

-Not obtained due to low resolution.

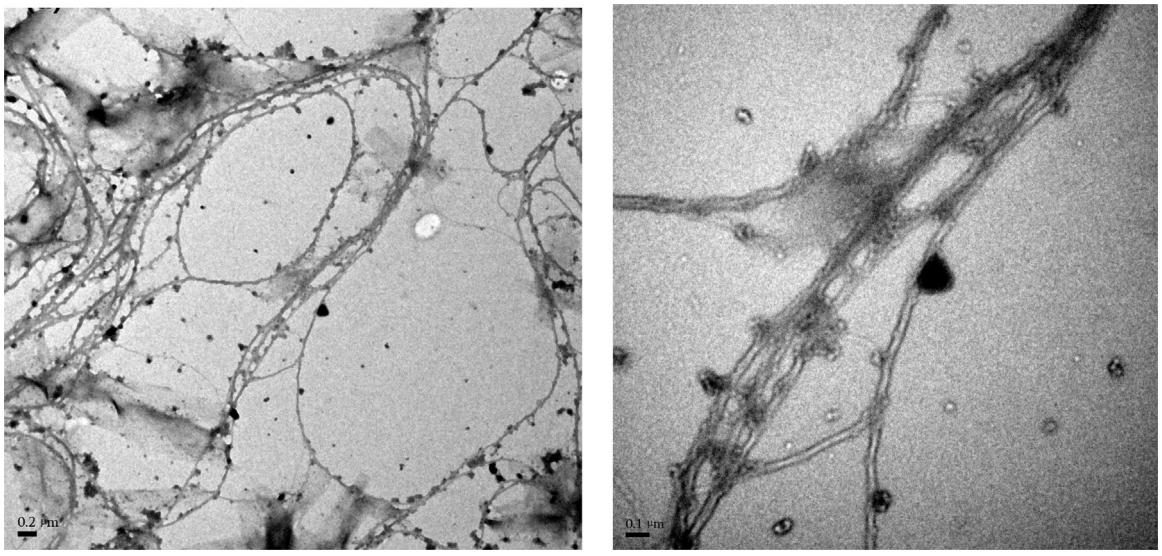


**Fig. 4.** TEM images of TSP-II in sodium dodecyl sulfate (SDS) solution.

of TSP-II displayed a broad stretching intense characteristic peak at approximately 3400 cm$^{-1}$ for the hydroxyl group, a weak C—H stretching band at approximately 2900 cm$^{-1}$, a monohydrate peak at approximately 1665 cm$^{-1}$ and a C—H variable angle vibration bond at approximately 1400–1200 cm$^{-1}$. The stretching peak at approximately 1100 cm$^{-1}$ suggested the presence of C—O bonds (Fig. 1b).

### 3.2. Periodate oxidation-Smith degradation

The polysaccharide TSP-II showed abundant $HIO_4$ uptake while it was oxidized. The consumption of $HIO_4$ (0.222 mmol) was more two times than the amount of formic acid (0.091 mmol) that was produced after 16 h of periodate treatment, indicating the little branch of TSP-II and the existing of monosaccharide which was 1 → linked, 1 → 6 linked, 1 → 2 linked, 1 → 2,6 linked, 1 → 4 linked or 1 → 4,6 linked. In addition, it should be concluded that sugar residues oxidized accounted for 42%. The periodate-oxidized products were hydrolyzed and examined by gas chromatography (Table 1). Four components mannose, xylose, galactose and glycerol were identified at a molar ratio of 3.1:0.95:1:0.58 in the fraction of full acid hydrolysis. The presence of large number of mannose and galactose indicated that their linkages could not be oxidized, namely (1 → 3)-glycosidic linkages. Xylose and glucose were little or absent, suggesting that they were all linkages that could be oxidized. In addition, glycerol was present, further suggesting that the following linkages of xylose and glucose existed: (1 → )-glycosidic linkages, (1 → 6)-glycosidic linkages, (1 → 2)-glycosidic linkages or (1 → 2,6)-glycosidic linkages.

### 3.3. Partial hydrolysis with acid

Four Fractions, obtained after partial acid hydrolysis of TSP-II, were subjected to GC analysis (Table 1). Both hydrolysis precipitation and precipitation in the sack contained mannose, xylose, galactose and glucose at a molar ratio of 6.9:3.4:1:1.25 and 3.4:1.7:1:0.23, respectively, indicating that they were the components of backbone structure of TSP-II. Mannose, xylose, glucose and galactose were also detected in other two fractions, indicating that they also could be in the position of branched structure of TSP-II.

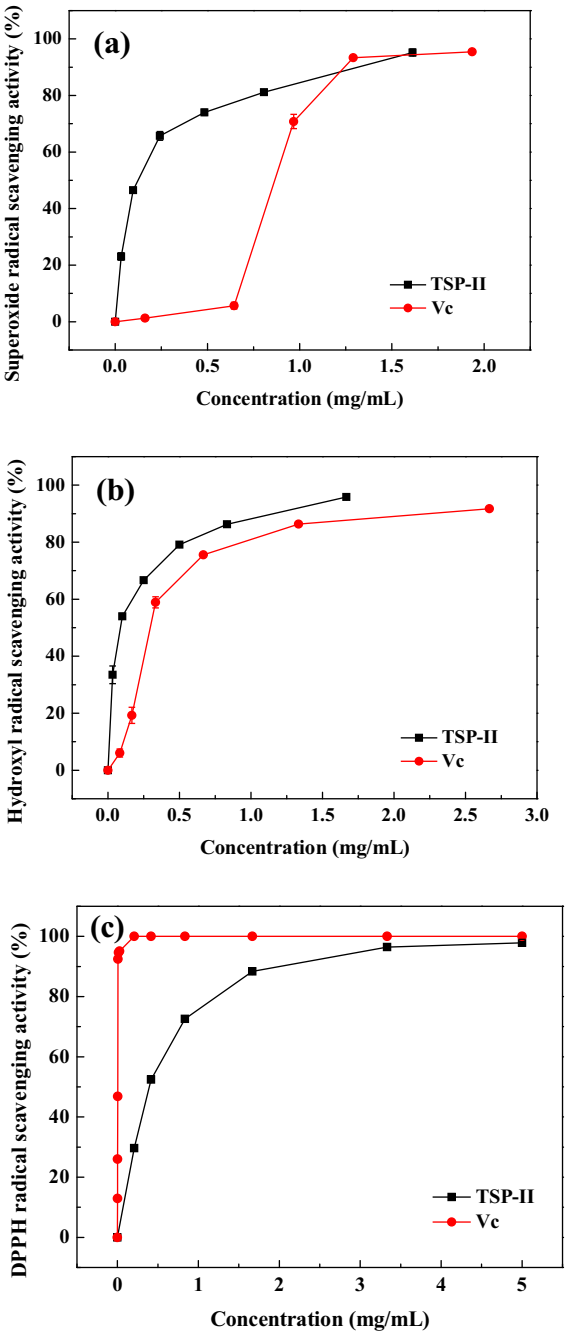


**Fig. 5.** Antioxidant activities of TSP-II: scavenging effects on (a) superoxide radical, (b) hydroxyl radical, and (c) DPPH radical.

### 3.4. Methylation analysis of TSP-II

The infrared spectrum of TSP-II displayed a broad stretching intense characteristic peak at approximately 3400 $cm^{-1}$ for the hydroxyl group. The FTIR spectrum of methylated TSP-II showed that the lack of an absorption peak of hydroxyl group identified the complete methylation. The methylation analysis of the TSP-II fraction showed the presence of four major components, namely 1,3,5-tri-*O*-acetyl-2,4,6-tri-*O*-methyl-D-mannitol, 1,2,5-tri-*O*-acetyl-3,4-di-*O*-methyl-D-xylitol, 1,5,6-tri-*O*-acetyl-2,3,4-tri-*O*-methyl-D-glucitol and 1,3,5-tri-*O*-acetyl-2,4-di-*O*-methyl-6-deoxy-D-galactiol in a molar ratio 4.45:0.8:1.31:1 (Table 2). The molar ratio from methylated derivatives was basically in accordance with the molar ratio of monosaccharide composition except xylose, and the losses of xylose could be induced by the sample treatment. In addition, the results from methylated analysis were in accordance with the results of periodate oxidation and smith degradation. The non-reducing terminals and the branched fraction of TSP-II were not identified in methylation, probably because their content was the least among residues or TSP-II was a non-branched polysaccharide.

### 3.5. NMR spectroscopy

$^{1}H$ (Fig. 2a), $^{13}C$ (Fig. 2b) and DEPT135 (Fig. 2c) NMR experiments were performed. Because they did not provide enough information about the anomeric configuration, a one-bond C-1-H-1 NMR experiment (HSQC) was completed (Fig. 3b). The $^{1}H$ NMR spectrum and HSQC spectra showed four signals in the anomeric region at $\delta$ 4.43, 4.9, 4.94 and 5.13 ppm. Four anomeric protons were attributed to four different types of glycosidic bonds. In the $^{13}C$ NMR, DEPT135 and HSQC spectrums, these four anomeric carbon signals appeared at $\delta$ 98.1, $\delta$ 100.4, $\delta$ 102.3 and $\delta$ 102.8 ppm, and all carbon chemical shifts were assigned. The four sugar moieties were designated as A, B, C and D according to their increasing chemical shifts (Table 3).

In the $^{1}H$ NMR spectrum of TSP-II, the chemical shift at 4.43 ppm was assigned to residue A. The corresponding chemical shift of this residue at 102.8 ppm in the $^{13}C$ NMR spectrum was confirmed by the HSQC spectrum. H-1, H-2, H-3 and H-4 were assigned to the shifts as shown in Table 3 according to the $^{1}H$–$^{1}H$ COSY spectrum. From the TOCSY spectrum, H-2, H-4 and H5 were confirmed. The corresponding $^{13}C$ chemical shifts of residue A could be assigned from the HSQC spectrum and were listed in Table 3. According to $^{13}C$ chemical shifts, this residue could be identified as →3)-α-D-Man*p*-(1→, and this assignment was consistent with the literature (Li, Wei, Sun, & Xu, 2006). Residue A was identified as →3)-α-D-Man*p*-(1→, its content was the largest in NMR, and these results were in accordance with the results of monosaccharide composition and GC–MS analysis.

The anomeric chemical shift for moiety B was at $\delta$ 4.9 ppm. The assignments of H-2 and H-3 of residue B could be obtained in the 2D-COSY spectrum, and chemical shifts of residue B (H-4, H-5, H-6) were confirmed by the correlation with H-1 in the TOCSY spectrum. The carbon signals from C-1 to C-6 for residue B were identified from the HSQC spectrum, and the anomeric carbon signal of residue B was seen at $\delta$ 98.1 ppm. According to its chemical shifts (Table 3), it was confirmed that residue B was →3)-α-D-Gal*p*-(1→, and this assignment was consistent with the literature (Pramanik, Mondal, Chakraborty, Rout, & Islam, 2005; Jing et al., 2015). The anomeric signals for moieties C and D were at $\delta$ 4.94 ppm and $\delta$ 5.13 ppm, respectively. The carbon chemical shifts from the C-1 to C-6 for residue C and residue D were assigned from the HSQC spectrum (Table 3). An anomeric proton signal was seen at δ~>5 ppm, and the $^{13}C$ signal for the anomeric carbon was observed at $\delta$ 99–102 ppm, which indicated that residues C and D were α-D-pyranose (Mondal, Chakraborty, Rout, & Islam, 2006; Rout, Mondal, Chakraborty, & Islam, 2006; Corsaro et al., 2005). The assignment of H-1 to H-5 of residue C and H-2 to H-3 of residue D could be obtained by cross peaks in the $^{1}H$–$^{1}H$ COSY spectrum, and chemical shifts of residue C (H-2, H-6) and residue D (H-3, H-4, H-5) were confirmed by the TOCSY spectrum. By comparing our results to the literature (Liu et al., 2015; Rout et al., 2006), residue C was identified as →6)-α-D-Glc*p*-(1→. The downfield shift of the C-6 carbon signal with respect to the standard values indicated that the C moiety was linked at this position. Residue D was assigned to the →2)-α-D-Xyl*p*-(1→, which was consistent with the literature (Chen, Liu, Zhang, Niu et al., 2015).

The sequence of glycosyl residues of TSP-II was determined via NOESY (Fig. 3d) and HMBC (Fig. 3e) experiments (Suarez et al., 2005). Residue A had an NOE contact from H-1 to H-2 of residue

D, in addition to intra-residue NOE contacts with H-2, H-4, H-5 and H-6. This indicated that residue A was linked at the 2-position of residue D, and the above NOE results suggested the following sequence between two residues of A and D.

→ 3)-α-d-Man*p*-(1 → 2)-α-d-Xyl*p*-(1 →

Residue D had an NOE contact from H-1 to H-3 of residue B, indicating that residue D was linked at position 3 of residue B. At the same time, residue B had an NOE contact from H-1 to H-6 of residue C. The following repeating unit was established.

→ 3)-α-d-Man*p*-(1 → 2)-α-d-Xyl*p*-(1 → 3)-α-d-Gal*p*-(1 → 6)-α-d-Glc*p*-(1 →

The peaks of residue A ($\delta$ 4.43) and residue D ($\delta$ 5.13) corresponded to six and three proportion of anomeric carbons of residue B ($\delta$ 4.9) or residue C ($\delta$ 4.94), respectively. These indicated that six residues A and three residues d were first linked, after which residues B and residues C was linked to them. Based on all of these findings, the repeating units present in polysaccharide TSP-II was determined to be the following:

→ [3)-α-d-Man*p*-(1]$_6$ → [2)-α-d-Xyl*p*-(1]$_3$ → 3)-α-d-Gal*p*-(1 → 6)-α-d-Glc*p*-(1 →

### 3.6. Molecular morphology of TSP-II

Morphological information is important to illustrate the fine structure of macromolecules intuitively (Chen, Liu, Zhang, Niu et al., 2015). Fig. 4 showed a portion of the particular TSP-II molecule with an extended conformation. Both non-branched conformations and entangled chains were observed from the TEM image of TSP-II in its fully extended state. This result was also in agreement with the results of methylation and NMR analyses that non-branched structure existed in TSP-II molecules. It has been reported that the entangled chain or helix conformation was beneficial for improving the antioxidant and antitumor activity of polysaccharides (Wang et al., 2015).

### 3.7. Antioxidant activities

On the basis of DPPH radical assay, superoxide radical assay and hydroxyl radical assay, antioxidant activities of TSP-II were investigated. The results of scavenging activities of Vc and TSP-II were presented in Fig. 5. $EC_{50}$ values of TSP-II for superoxide radical, hydroxyl radical and DPPH radical were 0.127 mg/ml, 0.088 mg/ml and 0.395 mg/ml, respectively, and $EC_{50}$ values of Vc for these radicals were 1.02 mg/ml, 0.396 mg/ml and 0.0027 mg/ml, respectively. The above results showed that scavenging activities of TSP-II for superoxide radical and hydroxyl radical were higher than Vc.

## 4. Conclusion

According to the results above, it was concluded that the crude polysaccharide TSP from *T. sanguinea* Peng contained predominantly a water-extractable polysaccharide (TSP-II, 31.56%) purified by DEAE Sepharose CL–6 B column chromatography. TSP-II consisted mainly of mannose, xylose, galactose and glucose at a molar ratio 5.9:2.4:1:1.1. The results of periodate oxidation-smith degradation, partial hydrolysis with acid, methylation linkage analysis and NMR of TSP-II indicated that →3)-α-D-Man*p*-(1→, →2)-α-D-Xyl*p*-(1→, →6)-α-D-Glc*p*-(1→ and →3)-α-D-Gal*p*-(1→ formed the major components of the main-chain structure. TSP-II was a non-branched heteropolysaccharide. TEM analysis revealed a primary on-branched and entangled microstructure. On the basis of antioxidant activities assay, $EC_{50}$ values of TSP-II on superoxide radicals and hydroxyl radicals were 0.127 mg/ml and 0.088 mg/ml, respectively, which were more pronounced than that of Vc.

It has been reported that the bioactivity of polysaccharides might be influenced by structural or physical features such as chain conformation (Wang et al., 2015). Notably, the non-branched structure and the entangled chain conformation of TSP-II might possess these valuable bioactivities (Chen, Liu, Zhang, Dai et al., 2015; Chen, Liu, Zhang, Niu et al., 2015).

## Acknowledgements

This work was supported by Promotion Program for Young and Middle-aged Teacher in Science and Technology Research of Huaqiao University (ZQN-PY316) and the National Nature Science Foundation of China (31201314).

## References

Bradford, M. M. (1976). Rapid and sensitive method for the quantitation of microgram quantities of protein utilizing the principle of protein-dye binding. *Analytical Biochemistry*, *72*, 248–254.

Chen, L., & Cheung, P. C. K. (2014). Mushroom dietary fiber from the fruiting body of *pleurotus tuber-regium*: fractionation and structural elucidation of nondigestible cell wall components. *Journal of Agricultural and Food Chemistry*, *62*, 2891–2899.

Chen, L., Zhang, B. B., Chen, J. L., & Cheung, P. C. K. (2014). Cell wall structure of mushroom sclerotium (*Pleurotus tuber-regium*): Part 2: Fine structure of a novel alkali-soluble hyper-branched cell wall polysaccharide. *Food Hydrocolloids*, *38*, 48–55.

Chen, L., Liu, J., Zhang, Y., Dai, B., An, Y., & Yu, L. (2015). Structural, thermal: and anti-inflammatory properties of a novel pectic polysaccharide from alfalfa (Medicago sativa L.) stem. *Journal of Agricultural and Food Chemistry*, *63*, 3219–3228.

Chen, L., Liu, J., Zhang, Y., Niu, Y., Dai, B., & Yu, L. (2015). A novel alkaline hemicellulosic heteroxylan isolated from alfalfa (*Medicago sativa* L.) stem and its thermal and anti-inflammatory properties. *Journal of Agricultural and Food Chemistry*, *63*, 2970–2978.

Corsaro, M. M., De Castro, C., Naldi, T., Parrilli, M., Tomás, J. M., & Regué, M. (2005). $^{1}$H and $^{13}$C NMR characterization and secondary structure of the K2 polysaccharide of *Klebsiella pneumoniae* strain 52145. *Carbohydrate Research*, *340*, 2212–2217.

Du, X. J., Zhang, J. S., Yang, Y., Ye, L. B., Tang, Q. J., Jia, W., et al. (2009). Structural elucidation and immuno-stimulating property of an acidic heteropolysaccharide (TAPA1) from *Tremella aurantialba*. *Carbohydrate Research*, *344*, 672–678.

Dubois, M., Gillis, K. A., Hamilton, J. K., Rebers, P. A., & Smith, F. (1956). Colorimetric method for determination of sugars and related substances. *Analytical Chemistry*, *28*, 350–356.

Jing, Y. S., Zhu, J. H., Liu, T., Bi, S. X., Hu, X. J., Chen, Z. Y., et al. (2015). Structural characterization and biological activities of a novel polysaccharide from cultured *Cordyceps militaris* and its sulfated derivative. *Agricultural and Food Chemistry*, *63*, 3464–3471.

Kiho, T., Kochi, M., Usui, S., Hirano, K., Aizawa, K., & Inakuma, T. (2001). Anti-diabetic effect of an acidic polysaccharide (TPA) from *Tremella aurantia* and its degradation product (TAP-H). *Biological & Pharmaceutical Bulletin*, *24*, 1400–1403.

Komura, D. L., Ruthes, A. C., Carbonero, E. R., Gorin, P. A. J., & Iacomini, M. (2014). Water-soluble polysaccharides from *Pleurotus ostreatus var*. Florida mycelial biomass. *International Journal of Biological Macromolecules*, *70*, 354–359.

Kumar, C. G., Joo, H. S., Choi, J. W., Koo, Y. M., & Chang, C. S. (2004). Purification and characterization of an extracellular polysaccharide from haloalkalophilic Bacillus sp. I-450. *Enzyme and Microbial Technology*, *34*, 673–681.

Li, B., Wei, X. J., Sun, J. L., & Xu, S. Y. (2006). Structural investigation of a fucoidan containing a fucose-free core from the brown seaweed, *Hizikia fusiforme*. *Carbohydrate Research*, *341*, 1135–1146.

Liu, X. Z., & Guo, C. J. (2009). Selection of liquid medium for Tremella sanguinea by L9(34) orthogonal design. *Edible Fungi of China*, *28*, 36–38.

Liu, J., Wen, X. Y., Kan, J., & Jin, C. H. (2015). Structural characterization of two water-soluble polysaccharides from black soybean (Glycine max (L.) Merr.). *Journal of Agricultural and Food Chemistry*, *63*, 225–234.

Luo, D. H., & Fang, B. S. (2008). Structural identification of ginseng polysaccharides and testing of their antioxidant activities. *Carbohydrate Polymers*, *72*, 376–381.

Luo, D. H., & Zeng, Y. W. (2014). Study on antioxidant activities of several extracts from tremella. *Natural Product Research and Development*, *26*, 284–286.

Luo, D. H., Yuan, X. M., Zeng, Y. W., Nie, K. Y., Li, Z. M., & Wang, Z. J. (2016). Structure elucidation of a major fucopyranose-rich heteropolysaccharide (STP-II) from Sargassum thunbergii. *Carbohydrate Polymers*, *143*, 1–8.

Luo, D. H. (2008). Identification of structure and antioxidant activity of a fraction of polysaccharide purified from *Dioscorea nipponica Makino*. *Carbohydrate Polymers*, *71*, 544–549.

Mondal, S., Chakraborty, I., Rout, D., & Islam, S. S. (2006). Isolation and structural elucidation of a water-soluble polysaccharide (PS-I) of a wild edible mushroom, *Termitomyces striatus*. *Carbohydrate Research*, *341*, 878–886.

Niu, Y., Shang, P., Chen, L., Zhang, H., Gong, L., Zhang, X., et al. (2014). Characterization of a novel alkali-soluble heteropolysaccharide from tetraploid gynostemma pentaphyllum makino and its potential anti-inflammatory and antioxidant properties. *Journal of Agricultural and Food Chemistry*, *62*, 3783–3790.

Peng, Y. B. (1990). A new species of the genus tremella from china. *Journal of Natural Science of Hunan University*, *13*, 253–256.

Pramanik, M., Mondal, S., Chakraborty, I., Rout, D., & Islam, S. S. (2005). Structural investigation of polysaccharide (Fr. II) isolation from the aqueous extract of an edible mushroom, Pleurotus sajor-caju. *Carbohydrate Research*, *340*, 629–636.

Rout, D., Mondal, S., Chakraborty, I., & Islam, S. S. (2006). The structure of a polysaccharide from fraction-II of an edible mushroom: pleurotus florida. *Carbohydrate Research*, *341*, 995–1002.

Suarez, E. R., Kralovec, J. A., Noseda, M. D., Ewart, H. S., Barrow, C. J., Lumsden, M. D., et al. (2005). Isolation: characterization and structural determination of a unique type of arabinogalactan from an immunostimulatory extract of Chlorlla pyrenoidosa. *Carbohydrate Research*, *340*, 1489–1498.

Wang, Z. J., & Luo, D. H. (2007). Antioxidant activities of different fractions of polysaccharide purified from *Gynostemma pentaphyllum* Makino. *Carbohydrate Polymers*, *68*, 54–58.

Wang, G. Y., Liang, Z. Y., Zhang, L. P., Miao, C. Y., Zhang, Y. S., & Fei, R. (2001). Studies on the structure of JS(1)-the water soluble polysaccharide isolated by alkaline from *Hippophae rhamnoides L. Chemical Journal of Chinese Universities-Chinese*, *22*, 1688–1690.

Wang, H., Qu, W., Chu, S., Li, M., & Tian, C. (2002). Studies on the preventive and therapeutic effects of the polysaccharide of Tremella aurantialba mycelia on diet-induced hyperlipidemia in mice. *Acta Nutrimenta Sinica*, *24*, 431–432.

Wang, Z. Y., Zhou, F., & Quan, Y. (2014). Antioxidant and immunological activity in vitro of polysaccharides from Phellinus nigricans mycelia. *International Journal of Biological Macromolecules*, *64*, 139–143.

Wang, K., Li, W., Rui, X., Li, T., Chen, X., Jiang, M., et al. (2015). Chemical modification, characterization and bioactivity of a released exopolysaccharide (r-EPS1) from Lactobacillus plantarum 70810. *Glycoconjugate Journal*, *32*, 17–27.

Xie, S. X., & Hu, C. W. (1992). Studies on biological characteristics of Tremella SP. *Edible Fungi of China*, *11*, 23–24.

Yuan, X., Zeng, Y., Nie, K., Luo, D., & Wang, Z. (2015). Extraction optimization characterization and bioactivities of a major polysaccharide from sargassum thunbergii. *Public Library of Science*, *10*(12), e0144773. http://dx.doi.org/10.1371/journal.pone.0144773

Zhang, W., Qu, W., & Zhang, X. (2004). The anti-hyperglycemic activity of polysaccharides from Tremella aurantialba mycelium. *Acta Nutrimenta Sinica*, *26*, 300–303.